

International Journal of Image and Graphics
© World Scientific Publishing Company

CONTOUR-POINT SIGNATURE SHAPE DESCRIPTOR FOR POINT CORRESPONDENCE *

ALEJANDRO J. GIANGRECO MAIDANA

Engineering School, National University of Asuncion, Paraguay. Email: ajgiangreco@gmail.com

HORACIO LEGAL AYALA

*Polytechnic School, National University of Asuncion. P.O.Box: 2111 SL. Central, Paraguay.
Email: hlegal@pol.una.py*

CHRISTIAN E. SCHAEERER

*Polytechnic School, National University of Asuncion. P.O.Box: 2111 SL. Central, Paraguay.
Email: cschaer@pol.una.py*

WALDEMAR VILLAMAYOR-VENIALBO

Centro Paraguayo de Informaciones Astronómicas, Asuncion, Paraguay. Email: wvenialbo@gmail.com

Received (Day Month Year)

Revised (Day Month Year)

Accepted (Day Month Year)

This article introduces a novel descriptor technique denoted as Contour-Point Signature useful to find correspondences of points selected from the outer contours of two arbitrary shapes, and to establish a relationship to map of an ordered sequence of contour's points from one shape to another. The proposal is proved to be invariant, to translation, scaling and rotation, it also induces a measure which is proved to be nonnegative, unique, symmetric and identity-preserving. Experimental tests were performed in shape detection under noise, with image retrieval from a MPEG-7 database and letter recognition. Numerical results show that the proposal is robust for noise perturbation, as well as, have adequate accuracy and hit rate, even with coarse tuning for its parameters. This makes the method attractive to a wide range of applications.

Keywords: contour; feature extraction; shape representation-alignment; signature

1. Introduction

Shape matching and point correspondence recovery play a fundamental role in many computer vision applications like object recognition, image database search, visual data mining, image retrieval, image registration and other related areas^{24,18,37,41}. There are several ways to carry out the shape matching task. Feature-based shape representation techniques allow the matching to be conducted in some approach-dependent feature

*This document dated December 8, 2016

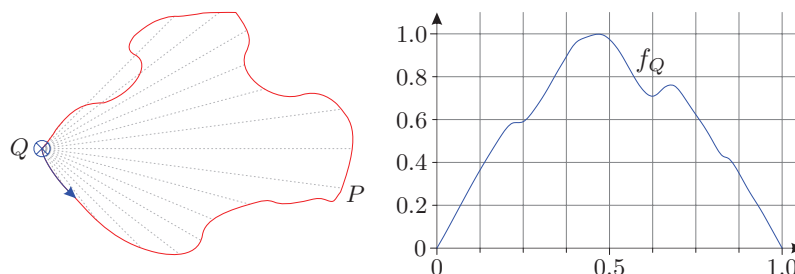
2 A. J. Giangreco-Maidana, H. L. Ayala, C. E. Schaerer, W. Villamayor-Venialbo

space, they mainly relies on shape descriptors. In contrast, in point-correspondence shape matching, the similarity between shapes is measured using point-to-point matching, i.e., every point on the shape is treated as a feature point, shape alignment is inferred by comparing points in the feature space, then, the shape matching process is conducted on 2-D space⁴⁵. An intermediate stage is the region-correspondence shape matching, in which the main shape is divided in smaller regional shapes, and each individual region, or a combination of them, is matched using feature-based techniques³⁸.

In the context of this work, a *shape descriptor* is a meaningful set of features produced to describe some given shape attributes, attempting to quantify the shape in ways that agree with human intuition and perception⁴¹. Those features are believed to carry discriminating and characterizing information about an object to be identified (for details see^{27,21,45}). By its turns, a *local descriptor* is the extension of that concept to smaller parts of a shape, for instance, a region, or even a point of the given shape. When dealing with local descriptors, the entire shape is represented by a set of local descriptors.

The identification of objects from imagery is not a trivial task¹, and many shape matching methods have been proposed in the past. Matching shapes in a manner that is independent of scale, position, and orientation is achieved by characterizing them with a set of extracted invariant features. Several techniques utilize moments to generate such invariant features^{13,17,33}. Other methods include curve matching¹⁶, active models⁸, curve evolution¹⁹, discriminative learning²⁵, shape matrix^{12,31}, shape context^{6,23}, skeletal context⁴⁰, algebraic and geometric approaches^{9,10,28}, Fourier descriptors^{5,43}, curvature scale space⁴⁴, graph matching^{4,7,32}, dynamic programming^{22,26}, and more. Further studies on shape matching are given in^{24,39,35,34,36}. Evaluation of shape descriptors for image retrieval is given in³. And an extensive overview of the current advances in pattern recognition is given in¹⁸.

In this work we propose a point (local) descriptor which is more expensive than a simple shape descriptor, however with broader applications. In this article it is used for contour matching, in this sense, the only descriptor comparable with Contour-Point Signature (CPS) found in the literature in the context of shape comparison is the shape context introduced at⁶. The CPS can be used to establish a relationship between any two set of points. In particular, as it is formulated in this article, relationships between rigid transformations of the sets of points (contour of images). We consider that this is an advantage. Our motivation for using a matching approach based on the outer contour of an object's shape, disregarding any internal holes and details, arises from the fact that it fulfills some important criteria¹¹ for good shape representation: (a) the contour remains unaltered under rigid geometric transformations, i.e., for shapes undergoing translation, scaling, and rotation; (b) it might match, to some extent, the human intuitive notion of shape similarity³⁰; (c) an object's contour remains invariant to extreme lighting conditions and large variations in texture or color²⁹; and (d) its understanding is not very difficult and its implementation not complicated. In fact, the outer contour of a shape captures most of the information about the object it represents; humans can easily identify objects and evaluate the similarity among them by just studying their silhouettes^{2,30}, even if they are incomplete^{14,15}. Therefore, using the contour to characterize an object

Figure 1. The contour-point signature f_Q for point Q .

is, in some way, in agreement with our visual perception, and can considerably reduce the amount of data to analyze, by discarding other information such as color, texture, etc.

This article is organized as follows: in §2 a theoretical foundation of the proposed descriptor is presented, with its construction and properties. In §3 a discretization of the CPS is presented, and we define the correspondence of points and shape matching for CPS. To this end, an induced metric, as well as, a dissimilarity measure are introduced and their theoretical properties are discussed. The good mathematical properties of the proposal are part of the novelty in this article, providing a theoretical framework for research in this direction. Numerical results are presented at §4 where the optimal sampling and the influence of noise perturbation in the data for the implementation efficiency of the proposal is analyzed. In addition, although the CPS can be used for many applications, in this paper examples are presented for image retrieval and letter recognition.

2. The Contour-Point Signature

Consider a given point Q on the contour of a 2-D shape, Figure 1, which is considered a simple closed curve, and start to rove along the contour in the counter-clockwise direction starting from point Q . For any other point P in the contour, distinct than Q , we associate the distance already traveled along the contour with the distance subtended by a line segment from Q to P ; i.e., we relate the arc-length s from Q to P with the length of the chord determined by these two points, discarding the chord orientation information. Although the definition of a 2-D shape is readily available in the literature — e.g.,²¹ or³⁴ — many times it has been stated in several flavors. Hence, it will be useful to include its definition in the context of this work, and a summary of some of its properties for the discussion to follow.

Definition 1. An object's *shape* is represented by a simply connected, two-dimensional compact set $\mathcal{F} \subset \mathbb{R}^2$, that is, a closed and bounded set of points from the plane \mathbb{R}^2 .

Definition 2. The *contour* $\Gamma(\mathcal{F}) \subset \mathcal{F}$ of a shape \mathcal{F} is a set of closed curves of the plane \mathbb{R}^2 formed by the points in the boundary of \mathcal{F} . Each one of these curves is smooth except in a finite number of points, i.e., it is formed by rectifiable Jordan's arcs.

The *silhouette* of an object is the set of points bounded by the *outer contour* of its shape,

4 A. J. Giangreco-Maidana, H. L. Ayala, C. E. Schaerer, W. Villamayor-Venialbo

which is the most external curve that encloses any other curve from the shape's contour. In this work, we will consider only the outer contour, that is to say, the silhouette's contour, though we will still noted it as $\Gamma(\mathcal{F})$. As has been defined above, this contour is considered piecewise smooth because it is expected the existence of corners on the borders of an object. The parametric functional for the contour is defined as follows.

Definition 3. The contour $\Gamma(\mathcal{F})$ of a silhouette \mathcal{F} is represented by the functional

$$\mathbf{x}(t): [0, 1] \mapsto \Gamma(\mathcal{F}), \quad (1)$$

one-to-one in the half-open interval $[0, 1)$ being $\mathbf{x}(1) = \mathbf{x}(0)$. The parameter t is the normalized arc-length such that the true arc-length $s = tp$, with $p = \int_{\Gamma(\mathcal{F})} ds = \int_0^1 |\mathbf{x}'(t)| dt$, that is, the length of the perimeter of the silhouette and $\mathbf{x}'(t) = d\mathbf{x}(t)/dt$.

To simplify the notation we consider the following conventions: (i) when expressing the contour functional as $\mathbf{x}(t)$ the parameter $t \in \mathbb{R}$ and $0 \leq t < 1$, i.e.,

$$t \equiv \begin{cases} t, & \text{if } 0 \leq t < 1; \\ t - \lfloor t \rfloor, & \text{otherwise;} \end{cases} \quad (2)$$

where $\lfloor \cdot \rfloor$ is the floor function, that is to say, the function that yields the largest integer number less than or equal to its argument; and (ii) any arbitrary point on the contour can be chosen as the starting point $\mathbf{x}(0)$, but once it has been chosen, it must be keep fixed during the whole analysis.

Now we formalize the generic concept of contour-point signature:

Definition 4. Given an object's silhouette \mathcal{F} , and an arbitrated point Q in its contour $\Gamma(\mathcal{F})$, i.e., $Q = \mathbf{x}(t_Q) \in \Gamma(\mathcal{F})$, $0 \leq t_Q < 1$; the *contour-point signature* (CPS) associated to Q , by $f_Q \in C_{[0,1]}$, is the continuous positive definite function, piecewise differentiable, bounded and compactly supported in $[0, 1]$ defined by:

$$f_Q(t) := \frac{1}{\|\mathcal{F}\|} |\mathbf{x}(t_Q + t) - Q|, \quad 0 \leq t \leq 1, \quad (3)$$

where $\|\mathcal{F}\|$ is a silhouette dependent norm devised to achieve the invariance to changes of scale, $|\cdot|$ is some underlying norm embedded in \mathbb{R}^2 , that is, the second factor of the right member of (3) is equivalent to an arbitrary distance function induced by such norm, and t_Q and t are normalized arc-lengths (defined at 2).

Note that f_Q is piecewise differentiable because $\Gamma(\mathcal{F})$, as defined previously, is piecewise smooth, and continuous since $\Gamma(\mathcal{F})$ is a closed curve. In addition, observe that the CPS captures the distribution of the length of the shortest path from that point to any other point along that contour, discarding the information about the path's trajectory. The choice of the norm $|\cdot|$ in (3) determine different CPS, for instance, the *Euclidean CPS* is obtained using the L_2 norm for computing distances in the expression (3). We can see immediately that contour-point signatures form a subspace of the normed space $C_{[0,1]}^*$, therefore, any metric induced for some norm that can be embedded in $C_{[0,1]}^*$ will serve to compare the closeness of contour's points in the contour-point space.

In addition with the characteristics already discussed, the CPS has the following properties.

Property 1. Starting point independence. Since the CPS for a point is related to the point itself, which point is selected as the starting point of the contour functional has no influence in the result.

Proof. A change of the starting point can be expressed as a shift of the parameter. Suppose that we displace the starting point by an amount Δt along the contour, such that $\hat{\mathbf{x}}(t) = \mathbf{x}(t + \Delta t)$ and $\hat{Q} = \hat{\mathbf{x}}(w)$. Consider also that $\hat{Q} \equiv Q = \mathbf{x}(u)$, *i.e.*, both represent the same point. Now,

$$\begin{aligned}
 f_{\hat{Q}}(v) &= \frac{1}{\|\mathcal{F}\|} |\hat{\mathbf{x}}(v+w) - \hat{Q}| && \dots \text{by definition} \\
 &= \frac{1}{\|\mathcal{F}\|} |\mathbf{x}(v+w+\Delta t) - Q| && \dots \text{by hypothesis} \\
 &= \frac{1}{\|\mathcal{F}\|} |\mathbf{x}(u+v) - Q| && \dots \text{ibidem} \\
 &= f_Q(v), && (4)
 \end{aligned}$$

which is the expression for the unshifted starting point, Equation (3). \square

Property 2. Invariance to translation. This property is inherent to CPS. Because a point from the shape is subtracted from the other boundary points, the signature values are relative distances, hence it is invariant to translation.

Proof. Suppose that we obtain a shape $\hat{\mathcal{F}}$ translating the shape \mathcal{F} by an amount \mathbf{z} , such that $\hat{\mathbf{x}}(t) = \mathbf{x}(t) + \mathbf{z}$, $\hat{Q} = \hat{\mathbf{x}}(u)$, and $Q = \mathbf{x}(u)$, then we have:

$$\begin{aligned}
 f_{\hat{Q}}(v) &= \frac{1}{\|\mathcal{F}\|} |\hat{\mathbf{x}}(u+v) - \hat{Q}| && \dots \text{by definition} \\
 &= \frac{1}{\|\mathcal{F}\|} |[\mathbf{x}(u+v) + \mathbf{z}] - [\mathbf{x}(u) + \mathbf{z}]| && \dots \text{by hypothesis} \\
 &= \frac{1}{\|\mathcal{F}\|} |\mathbf{x}(u+v) - \mathbf{x}(u) + \mathbf{z} - \mathbf{z}| && \dots \text{reordering} \\
 &= \frac{1}{\|\mathcal{F}\|} |\mathbf{x}(u+v) - Q| && \dots \text{substituting } Q \\
 &= f_Q(v), && (5)
 \end{aligned}$$

the same expression for the untranslated shape, equation (3). \square

Property 3. Invariance to rotation. As defined in (3), the parameter v relates each function value to the location of a fixed point on the contour, and therefore a rotation of the entire shape will not affect the relative positions of its points, the CPS is invariant to rotation.

6 A. J. Giangreco-Maidana, H. L. Ayala, C. E. Schaerer, W. Villamayor-Venialbo

Proof. Suppose that the shape \mathcal{F} is rotated by an angle θ by mean of the rotation matrix \mathbf{R}_θ , such that $\widehat{\mathbf{x}}(t) = \mathbf{R}_\theta \mathbf{x}(t)$, $\widehat{Q} = \widehat{\mathbf{x}}(u)$, and $Q = \mathbf{x}(u)$. Rotation matrices are unitary matrices then, as a consequence, $|\mathbf{R}_\theta \mathbf{x}| = |\mathbf{x}|$.

$$\begin{aligned}
 f_{\widehat{Q}}(v) &= \frac{1}{\|\mathcal{F}\|} |\widehat{\mathbf{x}}(u+v) - \widehat{Q}| && \dots \text{by definition} \\
 &= \frac{1}{\|\mathcal{F}\|} |\mathbf{R}_\theta \mathbf{x}(u+v) - \mathbf{R}_\theta \mathbf{x}(u)| && \dots \text{by hypothesis} \\
 &= \frac{1}{\|\mathcal{F}\|} |\mathbf{R}_\theta [\mathbf{x}(u+v) - \mathbf{x}(u)]| && \dots \text{factoring} \\
 &= \frac{1}{\|\mathcal{F}\|} |\mathbf{x}(u+v) - \mathbf{x}(u)| && \dots \text{substituting } Q \\
 &= f_Q(v), && (6)
 \end{aligned}$$

in other words, the original expression given by equation (3). \square

Remark Rotation invariance is not always desired because it makes signatures lose their discriminative ability if not measured relative to the same frame. Many applications in fact forbid rotation invariance, for instance, distinguishing a “6” from a “9”.

Considering that the signature values are purely geometrical, when searching for a shape’s norm we have many options to choose from, e.g., the shape’s perimeter length, the square root of its area, the longest chord in the shape, etc. Some of them may be more suitable than others in certain applications. It is important to remark that the CPS remains invariant under rigid transformations, i.e. it satisfy the Properties 2, 3 and 4. This means the CPS is similarity invariant.

Property 4. Scale invariance. According to (3), CPS is obtained by normalizing distances by an appropriate norm $\|F\|$ for the shape F .

Proof. Without loss of generality, suppose that the size of the shape \mathcal{F} is changed by a scale factor of $k > 0$, such that $\widehat{\mathbf{x}}(t) = k \mathbf{x}(t)$, $\widehat{Q} = \widehat{\mathbf{x}}(u)$, and $Q = \mathbf{x}(u)$. Let us take the perimeter length as the norm, i.e. $\|\mathcal{F}\| = p$ and $\|\widehat{\mathcal{F}}\| = \widehat{p}$, but $\widehat{p} = \int_0^1 |\widehat{\mathbf{x}}'(t)| dt = k \int_0^1 |\mathbf{x}'(t)| dt = kp$. Also consider that $|k\mathbf{x}| = k|\mathbf{x}|$. Then

$$\begin{aligned}
 f_{\widehat{Q}}(v) &= \frac{1}{\widehat{p}} |\widehat{\mathbf{x}}(u+v) - \widehat{Q}| && \dots \text{by definition} \\
 &= \frac{1}{kp} |k\mathbf{x}(u+v) - k\mathbf{x}(u)| && \dots \text{by hypothesis} \\
 &= \frac{1}{kp} |k[\mathbf{x}(u+v) - \mathbf{x}(u)]| && \dots \text{factoring} \\
 &= \frac{k}{kp} |\mathbf{x}(u+v) - \mathbf{x}(u)| && \dots \text{by hypothesis} \\
 &= \frac{1}{p} |\mathbf{x}(u+v) - \mathbf{x}(u)| && \dots \text{simplifying} \\
 &= f_Q(v), && (7)
 \end{aligned}$$

which is analogous to the expression given by equation (3). \square

3. The discrete CPS - descriptor

In this action we consider the image as a set of points (pixels) ordered in a matrix form and the shape as a subset of it. Consider its contour \mathcal{A} and some reference points on it denoted as $\mathcal{P} = \{P_1, \dots, P_N\}$, $P_i \in \mathbb{R}^2$ (see Figure 2). Given an arbitrary point P_0 , the discrete CPS is defined as follow

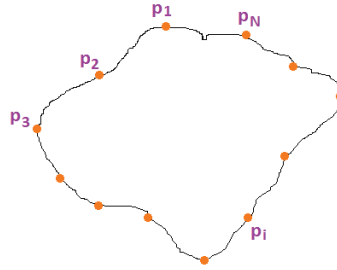


Figure 2. Reference points in the contour

$$f_{p_i}(j) = \frac{1}{\|\mathcal{A}\|} |p_i - p_{r(j)}|, \quad \begin{cases} r(j) = i, i + 1, \dots, N, 1, 2, \dots, i \\ j = 1, 2, \dots, N + 1 \end{cases}$$

where $\|\mathcal{A}\|$ is a convenient norm. In this work we adopt for $\|\mathcal{A}\|$ the square of the area formed by the polygon with vertices points \mathcal{A} . The discrete CPS is shown in Figure 3.

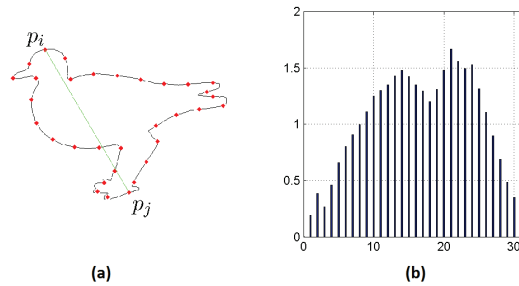


Figure 3. CPS f_{p_i} for the point p_i (b) and the relative chord of points p_i and p_j (a)

The Contour point signature can identify an specific point in the contour. This however is not enough to characterize the complete contour. If it is desired to have an unique

8 A. J. Giangreco-Maidana, H. L. Ayala, C. E. Schaerer, W. Villamayor-Venialbo

descriptor for the contour, this is desired, take the CP signature for each of the points in \mathcal{P} that describe discretely the contour. As a result it is obtained a matrix denoted as FPC (feature countour point) where each column corresponds to a CP for an specific point. Although FPC matrix can be assembled, in the context of this work we avoid to assemble this matrix and use directly the CPS for the points in \mathcal{P} .

Given two contours \mathcal{A} y \mathcal{B} , with their corresponding reference points $\mathcal{P} = \{p_1, \dots, p_N\}$ and $\mathcal{Q} = \{q_1, \dots, q_N\}$, respectively. We seek for a correspondence between \mathcal{P} and \mathcal{Q} . Hence, it is necessary to find a $j \in \mathbb{N}$, such that $\{p_1 \rightarrow q_j, p_2 \rightarrow q_{j+1} \dots\}$ where \rightarrow means the correspondence of points. The correspondence of points between two shapes is mainly important in the case of similar shapes with a rotation of one with respect to another. We are interested in seeking a rotation to better relate the points between the shapes. This is an linear with restriction assignment problem. To this end, consider a point $p_i \in \mathcal{P}$ and $q_j \in \mathcal{Q}$. The cost matrix C is defined by its entries $C_{i,j} = d(f, g)$ being the distance between two descriptors f and g . Any distance function can be used for $d(f, g)$; in the context of this work we use R -measure introduced before. Hence, the cost matrix C takes the form:

$$C = \begin{pmatrix} d(f_1, g_1) & d(f_1, g_2) & \dots & d(f_1, g_N) \\ d(f_2, g_2) & d(f_2, g_3) & \dots & d(f_2, g_1) \\ \vdots & \vdots & \vdots & \vdots \\ d(f_N, g_N) & d(f_N, g_1) & \dots & d(f_N, g_{N-1}) \end{pmatrix}$$

$$= [d(f_i, g_{\pi(i,j)})]_{ij}$$

and the correspondence problem is set as to find \hat{j} which minimize the functional cost defined as follows:

$$H(j) = \sum_{i=1}^n d(f_i, g_{\pi(i,j)}) \quad j = 1, 2, \dots, n \quad (8)$$

where $\pi(i, j) = (i + j - 2) \bmod(N) + 1$ is a rotation. Then, the correspondence problem can be summarizes as

$$H(\hat{j}) = \min_{j=1, \dots, n} \{H(j)\}, \quad (9)$$

and it is equivalent to find the column j (denoted by \hat{j}) in the cost matrix C with minimum $\sum_i C_{i,j}$, since each column represents a rotation.

3.1. Correspondence of points

In Figure 4 it can be seen the contour in blue and its reference points in red (in a illustrative way, N is small), and where $\hat{j} = 6$. Figure 5 shows the cost functional $H(j)$ relative to the shapes in 4 (with $N = 10$). Clearly the minimum of $H(j)$ corresponds to $\hat{j} = j = 6$.

In Figure 6 it is show a geometrical interpretation the equivalence between a rotation and each column of the cost matrix. Observe that each column of the cost matrix is equivalent to a rotation of shape \mathcal{B} . Figure 6 (a) shows the shape \mathcal{B} in its original position which

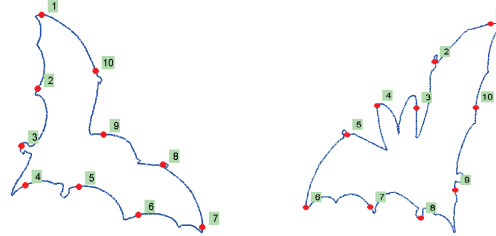
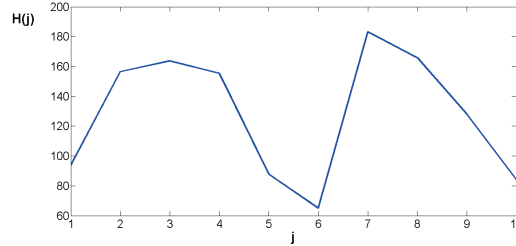


Figure 4. Correspondence of points

Figure 5. Function $H(j)$. The minimum of $H(j)$ at $j = 6$.

corresponds to the first column of the cost matrix. Figure 6 (b) shows a simple rotation (one step), corresponding to the second column of the cost matrix.

It is important to remark that occasionally it is not necessary to compare at each rotation all points, but only a fraction of them. We quantify this using a parameter δ , so $\delta = 1$ means the comparison of all points while $\delta = 0.5$ the comparison of half of them. This parameter affects directly to the efficiency of the method, as well as, the computational complexity (execution time). Hence, the cost function takes the form:

$$H(j) = \sum_i d(f_i, g_{\pi(i,j)}) \quad (10)$$

for each $i = 1, 1 + (1/\delta)N, \dots, 1 + (k/\delta)N, \dots, N$ and $j = 1, 2, \dots, N$, and where δ needs to be determined.

In addition, in many cases only small rotations of the original shapes must be considered. For instance, if we are interested to identify digits, if all possible rotations are considered, the number '6' will be identical to the number '9'. Hence in such a case, it is necessary to consider only the first and last columns of the cost matrix C . This equivalent to consider only small rotations of the image with respect to the original image. The number of rotations is given by the parameter γ , where $\gamma = 1$, implies to consider all rotations, while $\gamma = 0.5$ implies to consider only half of them. In Figure 7 can be observed these variants.

Figure 8(b) shows several cost functions $H(j)$ (associated to different δ values) rela-

10 A. J. Giangreco-Maidana, H. L. Ayala, C. E. Schaerer, W. Villamayor-Venialbo

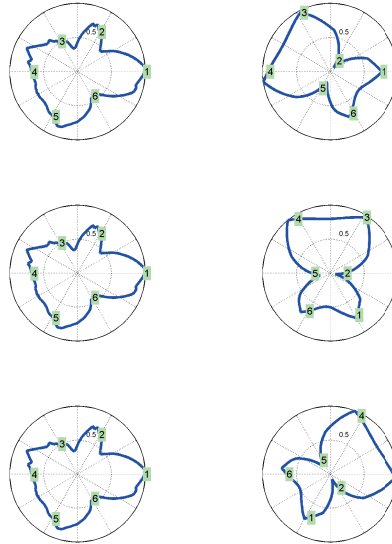


Figure 6. Interpretation of the cost matrix C . The first three rotations are presented.

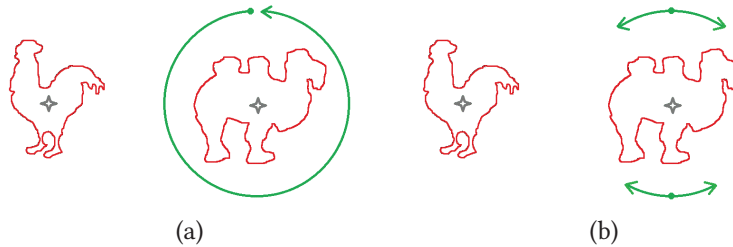


Figure 7. Interpretation of γ - parameter: (a) all rotations, (b) γ rotations around the original shape.

tives to Figure 8 (a) (with $N = 128$). Observe that even with $\delta = 0.0625$ the value of \hat{j} is correctly identified.

In case of rigid rotation there exist a correspondence is a simple rotation, although in general, this is not the case. As it can be seen in Figure 4, where the correspondence it is not a simple rotation. In addition, the cost matrix with the CPS C allows to find a correspondence of points and a geometrical transformation between two shapes. In addition the cost function H induces a dissimilarity measure. Both concept are going to be discussed in the following section.

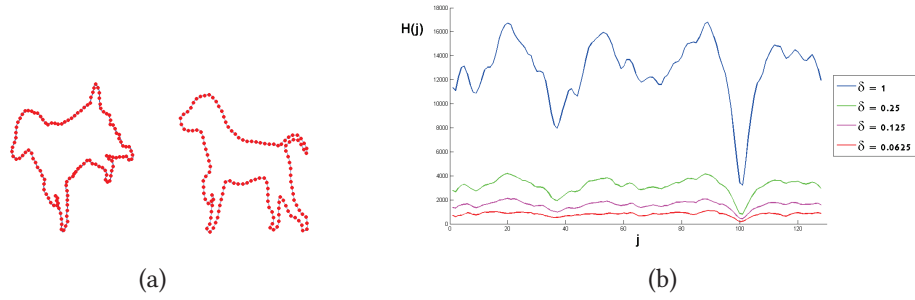


Figure 8. (a) Two figures of dog with $N = 128$. (b) Cost functions $H(j)$ for $N = 128$ and several values of δ .

3.2. Affine transformation

Once the correspondence of points have been performed, to compare two contours \mathcal{A} y \mathcal{B} , with reference points $\mathcal{P} = \{p_1, \dots, p_N\}$ and $\mathcal{Q} = \{q_1, \dots, q_N\}$, respectively; we use a transformation ⁶. This is done to overlap the contour allowing us to measure the similarity between them. An example it can be seen at Figure 9. There are several kind of transformations that can be implemented. By simplicity, and since this part is not in the scope of the article we use a homogeneous coordinate affine transformation which is modeled by $\mathbf{y} = T\mathbf{x}$. The matrix T is obtained from matrices Q and P by $T = QP^*$. The entries of P and Q are the coordinates of \mathcal{P} and \mathcal{Q} , respectively; and they have the form:

$$P = \begin{pmatrix} 1 & p_{11} & p_{12} \\ \vdots & \vdots & \vdots \\ 1 & p_{N1} & p_{N2} \end{pmatrix} \quad Q = \begin{pmatrix} 1 & q_{11} & q_{12} \\ \vdots & \vdots & \vdots \\ 1 & q_{N1} & q_{N2} \end{pmatrix}$$

and $P^* = P^t(PP^t)^{-1}$ is the pseudo inverse of P . There are other transformations that

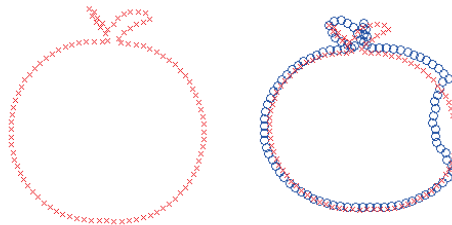


Figure 9. In the left: original contour \mathcal{A} . In the right: Contour \mathcal{B} (blue) and the contour transformed $\mathcal{T}(\mathcal{A})$ (red).

can be implemented.

12 A. J. Giangreco-Maidana, H. L. Ayala, C. E. Schaerer, W. Villamayor-Venialbo

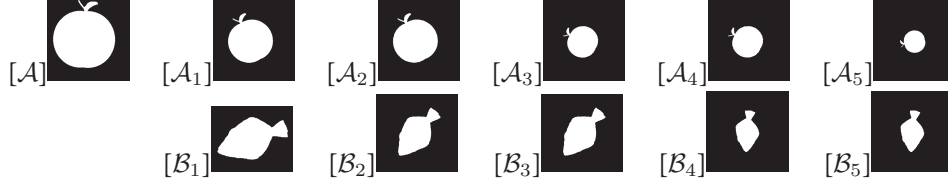


Figure 10. Example of a group of test images.

3.3. Dissimilarity measure

The numerical value used to qualify the dissimilarity between two shapes we denote as dissimilarity metric, varying proportionally to the dissimilarity of the contours. The matrix H induces a metric distance function denoted by $d_{CPS}(\mathcal{A}, \mathcal{B})$. Analogously, the affine transformation induces a metric distance function $d_T(\mathcal{A}, \mathcal{B})$.

3.3.1. Induced correspondence of points metric

The similarity metric function induced by the correspondence of points between \mathcal{A} and \mathcal{B} through the function H (introduced in Section 3.1) is given by

$$d_{CPS}(\mathcal{A}, \mathcal{B}) = H(\hat{j}) = \sum_i d(f_i, f_{\pi(i, \hat{j})}), \quad (11)$$

being the minimum if the cost function defined (8). $d_{CPS}(\mathcal{A}, \mathcal{B})$ has following properties:

Nonnegativity $d_{CPS}(\mathcal{A}, \mathcal{B}) \geq 0$.

$$\begin{aligned} d_{CPS}(\mathcal{A}, \mathcal{B}) &= H_1(\hat{j}) \\ &= \sum_i d(f_i, g_{\pi(i, \hat{j})}) && \dots \text{by definition} \\ &\geq 0 && \dots \text{positive terms.} \end{aligned}$$

Identity $d_{FCP}(\mathcal{A}, \mathcal{B})$ is reflexive, i.e. $d_{CPS}(\mathcal{A}, \mathcal{A}) = 0$.

$$\begin{aligned} d_{CPS}(\mathcal{A}, \mathcal{A}) &= H_1(\hat{j}) \\ &= \sum_i d(f_i, f_{\pi(i, \hat{j})}) && \dots \text{by definition} \\ &= \sum_i d(f_i, f_i) && \dots \text{for } j = 1 \\ &= 0 && \dots \text{zero terms.} \end{aligned}$$

Uniqueness $d_{CPS}(\mathcal{A}, \mathcal{B}) = 0$ implies $\mathcal{A} = \mathcal{B}$.

$$\begin{aligned} d_{FCP}(\mathcal{A}, \mathcal{B}) &= 0 \\ &= \sum_i d(f_i, g_{\pi(i, \hat{j})}) && \dots \text{by definition} \end{aligned}$$

implying

$$d(f_i, g_{\pi(i,j)}) = 0 \quad \forall i = 1, 2, \dots, N \quad \dots (d \text{ is positive})$$

finally

$$d(f_i, g_{\pi(i,j)}) = 0 \rightarrow f_i = g_{\pi(i,j)} \rightarrow \mathcal{A} = \mathcal{B}.$$

Symmetry $d_{FCP}(\mathcal{A}, \mathcal{B}) = d_{FCP}(\mathcal{B}, \mathcal{A})$. It is enough to observe that the columns of the cost matrices associated to $d_{FCP}(\mathcal{A}, \mathcal{B})$ and $d_{FCP}(\mathcal{B}, \mathcal{A})$ have the same entries but with different ordering. As a consequence, their corresponding matrices H have the same values but with different ordering.

$$\begin{aligned} d_{CPS}(\mathcal{A}, \mathcal{B}) &= \sum_i d(f_i, g_{\pi(i,j)}) && \dots \text{by definition} \\ &= \sum_i d(f_{\pi(i,j)}, g_i) && \dots \text{ordering the terms} \\ &= \sum_i d(g_i, f_{\pi(i,j)}) && \dots \text{by hypothesis} \\ &= d_{CPS}(\mathcal{B}, \mathcal{A}). \end{aligned}$$

3.3.2. Induced affine transformation metric

Using the affine transformation we define the following metric

$$d_T(\mathcal{A}, \mathcal{B}) = \|Q - TP\|_* = \sum_{i=1}^N \sum_{j=1}^3 [Q - TP]_{ij} \quad (12)$$

where $\|\cdot\|_*$ corresponds to the sum of the entries of the matrix (entrywise norm). This expression indeed the similarity of the contours represented by its points of reference. The computed value is the sumatory of the distances of the points Q (associated to the shape \mathcal{B}) and the corresponding points TP (associated to the shape \mathcal{A} after the transformation T). This metric is positive, reflexive and non-discernible but it is not symmetric.

Although the metric induced by the affine transformation is not symmetric, experimentally it is observed certain symmetry and in many cases symmetry is not required³⁶. In the context of this work we explore the convex combination ($\alpha + \beta = 1$) of the induced metrics defined above the

$$d(\mathcal{A}, \mathcal{B}) = \alpha d_{CPS}(\mathcal{A}, \mathcal{B}) + \beta d_T(\mathcal{A}, \mathcal{B}). \quad (13)$$

Hence given a tolerance parameter threshold τ and the metric $d(\mathcal{A}, \mathcal{B})$, two shapes \mathcal{A} y \mathcal{B} are similar if $d(\mathcal{A}, \mathcal{B}) < \tau$.

4. Computational Results

The computation of the similarity between two shapes \mathcal{A} and \mathcal{B} has the followings steps: the selection of the discretization number N of reference points in both contours, the

14 A. J. Giangreco-Maidana, H. L. Ayala, C. E. Schaerer, W. Villamayor-Venialbo

Table 1. Error when N and α change. In bold is denoted the best N which corresponds to the minimal error for a predefined parameter α .

	$N = 32$	$N = 64$	$N = 112$	$N = 128$	$N = 160$	$N = 256$	$N = 320$
$\alpha=0$	0.1625	0.0875	0.0500	0.0375	0.0500	0.0125	0.0250
$\alpha=0.1$	0.1625	0.0875	0.0500	0.0375	0.0375	0.0125	0.0250
$\alpha=0.25$	0.1625	0.0750	0.0500	0.0375	0.0375	0.0125	0.0125
$\alpha=0.5$	0.1375	0.0625	0.0500	0.0375	0.0250	0.0125	0.0125
$\alpha=0.75$	0.1250	0.0500	0.0250	0.0250	0.0125	0.0125	0.0125
$\alpha=0.9$	0.1250	0.0500	0.0250	0.0125	0.0125	0.0125	0.0125
$\alpha=1$	0.0375	0.0000	0.0000	0.0000	0.0000	0.0000	0.0000

computation of the respective CPS, the correspondence of points, the affine transformation and finally, the computation of the dissimilarity function. In the experiments we use the data base MPEG-7 created by the Moving Picture Experts Group which is used normally to evaluate algorithms for pairing images.

4.1. Optimal sampling number N , threshold τ and error E

In this section, we perform experiments with a training set obtained by selecting some pairs of figures from the standard data base MPEG-7²⁰. To this end, 40 groups of images are generated. Each group contain a image \mathcal{A} and 5 variations of it ($\mathcal{A}_1, \mathcal{A}_2, \mathcal{A}_3, \mathcal{A}_4, \mathcal{A}_5$) and other variations $\mathcal{B}_1, \mathcal{B}_2, \mathcal{B}_3, \mathcal{B}_4$ and \mathcal{B}_5 of the image \mathcal{B} different of \mathcal{A} . An example of a group of images are shown in Figure 10. For each N we compute the distances $d_{\mathcal{A}}(i) = d(\mathcal{A}, \mathcal{A}_i)$ and $d_{\mathcal{B}}(i) = d(\mathcal{A}, \mathcal{B}_i)$. We use the distance between similar images as $d_A = \max\{d_{\mathcal{A}}(i)\}$ and the distance between different images as $d_B = \min\{d_{\mathcal{B}}(i)\}$. It is possible to take images more different for the similar class of images and take the mean instead of max and min.

The computed distances are shown at Figure 11 where the distances corresponding to similar images are depicted as blue circles while those corresponding to different images are shown as red crosses for each of the 40 groups of images generated. The objective is to chose N and a threshold τ to better separate (with a green line in Figure 11) these two sets of points (in blue and red). This is obtained minimizing the error given by

$$E = \frac{FP + FN}{2 \times 40}, \quad (14)$$

where FP (*false positives*) is the number of similar images considered different due to the threshold chosen (equivalently it is the number of blue points above the green threshold line in Figure 11). FN (*false negative*) is the number of different images considered similar due to the threshold chosen (equivalently it is the number of red points below the green threshold line in Figure 11). Hence we consider the error as the quotient between the number of computed wrong distances and the total number of possible distances considered.

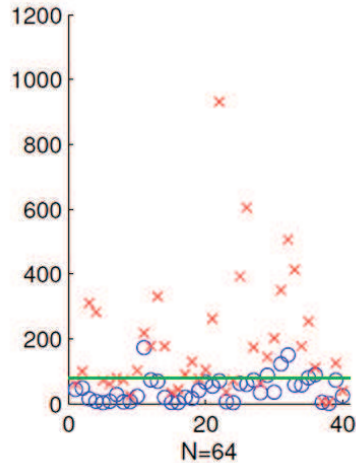


Figure 11. Distance between similar images and different images for $N = 64$. Similar image distance denoted in blue (O), and different image distance in red (X)

Table 1 shows the error given by (14) as a function of α and N using $\delta = 1$ and $\gamma = 1$. Observe that for a specific α there is a number N which minimizes the error (14).

4.2. The effect of noise

To evaluate the robustness of the proposal we use several levels of noise in the contour of the shape in the image. We consider the MPEG-7 CE-Shape-1 database which consists in 70 classes with 20 images every one. We divide in 20 sub-databases; in each one, there are 70 shapes from the 70 different classes according to their orders in the database. For every level of noise, every shape is perturbed by normal noise, an example is shown in Figure 12. For every sub-database, we take one perturbed shape as a query and we compute its distances with all the unperturbed shapes of the same subdatabase; if our method can correctly identify the similar shape, then it is considered as a successful event.

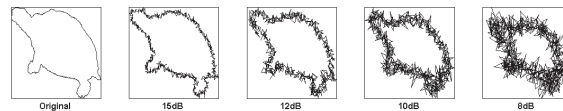


Figure 12. Contour with several levels of noise

An example is presented at Figure 13. We repeat this procedure for all shapes of the sub-database and for all sub-databases. Thus, the best possible result is 70 in every sub-database for each noise level.

16 A. J. Giangreco-Maidana, H. L. Ayala, C. E. Schaerer, W. Villamayor-Venialbo

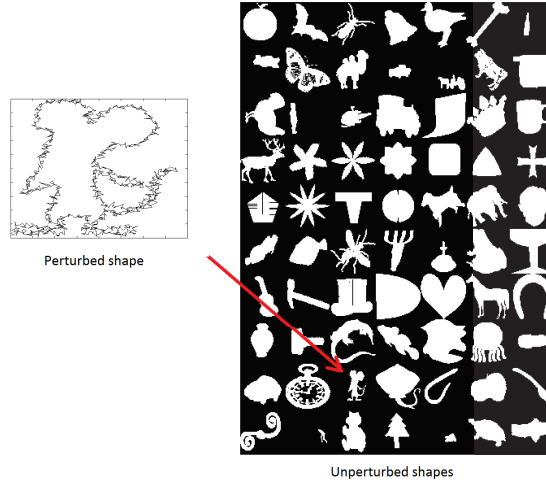


Figure 13. Comparison between a perturbed shape and its unperturbed sub-database.

Each perturbed images of each group is imposed to 15, 12, 10 and 8 dB noise levels. Every point of the contour of the image is affected by the noise. The perturbation in the contour is performed imposing a noise with normal distribution of mean μ and standard deviation σ at each cartesian axis. The parameter μ is computed using $\mu = (\sum_{i=1}^m \|p_i - c\|)/m$ where $\{p_i \in \mathbb{Z}, i = 1, \dots, m\}$ is the set of reference points p_i in the contour and c is the centroid of the figure; i.e., μ is the mean distance of all reference points p_i of the contour to the centroid c . The standard deviation σ is given by the expression:

$$\sigma = \frac{\mu}{SNR}, \tag{15}$$

where SNR is the Signal Noise Ratio defined by the expression $SNR_{dB} := 10 \log_{10} SNR$.

We also want to explore the sensitiveness of the identification system with respect to the fraction of comparison points δ at matching step (see §3.1). To this end, we consider $\delta = 0.0625$ and $\delta = 0.03125$ (which corresponds to consider only approximately 6% and 3% of the total of reference points, respectively).

Table 2. Effectiveness (in %) face to noise perturbations. $CPSM(N, \alpha, \delta)$.

Noise (in dB)	15.00	12.00	10.00	8.00
CPSM (128, 0.3, 0.03125)	99.35	98.42	97.35	90.57
CPSM (64, 0.3, 0.0625)	99.35	98.42	96.00	86.35
CPSM (128, 1, 0.03125)	99.42	97.35	87.92	60.28
CPSM (64, 1, 0.0625)	99.07	96.71	87.00	58.57
Chord Context ⁴²	82.90	-	-	-

Table 2 presents the effectiveness measured as the number of correct identified image in comparison with respect to the total of images that can be identified. As it can be observed the for the number of sampled points N and the level of noise tested, the best results are obtained for $\alpha = 0.3$, and it is enough in this case to use a value of δ just only of 0.03125. Observe also that in contraposition with the results obtained at §4.1, when a larger value of α minimize the error, in this case, smaller values of α make the method robust in front to noise. Observe that the performance of the identification system for $\delta = 0.03125$ has an effectiveness of 90.57% (with $\alpha = 0.3$) in the worse case scenario which is a quite good result. Notice that for a fixing α , considering half of N and duplicating δ to the value 0.0625 the results are quite similar (compare rows 1 and 2, and 3 and 4 of Table 2, respectively), but it takes only the half time for the computation.

4.3. Image retrieval system

The performance of an image retrieval system is normally tested taking an arbitrary image (consulting image) and computing the distance from this image to the rest of the images of the data base. Afterwards the images are ordered based on the distance to the consulting image.

In this experiment, we use the MPEG-7 data base, which contains binary images grouped in classes in accordance to certain characteristics of the image; for instance, the category car includes several images based on the same concept (cars) but with differences in their corresponding contours. There are 1400 images divided in 70 categories, and each category has 20 images. The data base is available freely ^a. For his experiment, we use $\alpha = 0.3$, $N = 128$, $\delta = 0.03125$, $\gamma = 1$ and the d_{CPS} as the distance function for the correspondence of points.

We use the Bull Eye Percentage (BEP) test which is computed considering the correct images identified between the 40 closer neighbor images. Notice that the possible maximum value for each image is 20, therefore the number of total possible correct image matches is $20 \times 1400 = 28000$. Considering all images, we obtain a retrieval rate of 70.72 %. We consider this number imply a very good performance of the technique since that any technique for enhancing the retrieval, such as multi resolution or adaptive techniques, have been used and only a fraction of the reference points have been taken into account.

We also study the retrieval rate behavior while the number of classes is reduced (rBEP). At each step, classes with worst performance on the previous step are eliminated. Results are presented at Table 3. As we can see, the performance is improved in a linear way between 54 and 30 classes. We consider that our method achieves good results considering this database is very heterogeneous (it contains non rigid shapes, shapes with internal contour).

For analyzing the sensibility of the rate of retrieval of the method as a function of α , we randomly fix 5 classes (butterfly, hammer, car, spoon and spring) while α varies. Two

^a<http://www.dabi.temple.edu/shape/MPEG7/dataset.html>

18 *A. J. Giangreco-Maidana, H. L. Ayala, C. E. Schaerer, W. Villamayor-Venialbo*

Table 3. *rBEP (reduced BEP) variation with respect to the number of classes with $N = 128$.

Number of classes (best)	54	43	38	30
rBEP*	74.73	84.65	88.15	93.52

Table 4. Variation of *rBEP (reduced BEP) with respect to α . Computed with only 5 classes and $N = 128$.

α	0.1	0.25	0.5	0.75	0.9
rBEP*	79.7000	80.2500	82.9500	87.0000	87.7000
α	0.8	0.85	0.9	0.95	1
rBEP*	87.3000	88.4000	87.7000	89.2000	90.5000

Table 5. Effectiveness (in %) face to Letter recognition

α	0	0.30	0.50	0.70	0.85	1.00
N=32	72.222222	76.353276	81.054131	87.037037	87.321937	85.612536
N=64	71.937322	78.347578	85.470085	88.603989	88.603989	86.182336
N=128	72.222222	80.911700	86.894587	88.746439	88.603989	86.182336
N=256	72.364672	83.618234	88.034188	88.888889	89.031339	86.324786

tables are presented. Table 4 shows the rBEP variation with respect to a large variation of α and the results of the rBEP variation as a function of α around $\alpha = 0.9$.

It can be observed that the best response of the method for image retrieval it is obtained in this experiment for a value of $\alpha = 1$ with a value of rBEP= 90.5. This experiment denotes that the choice of the parameter α depends on the problem.

4.4. Letter recognition

In this section we test the CPS method for an letter recognition application. For this purpose, we generate two different datasets. The first one, a reference dataset, which consists in 26 shapes of the alphabet. The second one is a test dataset consisting in the alphabet and variations of them, making a total of $26 \times 27 = 702$ shapes (27 variations of every letter). See Figures 14 (a) and (b). The experiment consists of taking a shape from test dataset and comparing it with all reference shapes. If the closest reference shape corresponds to the same letter, then it is considered as a successful match. We repeat for all the test shapes and, thus, the best result possible is 702.

Table 5 shows the performance for every letter under the best parameters. The parameters were considered as $\delta = 1$ and $\gamma = 0.25$. We obtain a best performance of 89.03% for a value of $\alpha = 0.85$ and $N = 256$.

Figure 15 shows the rates of recognition for each letter involved in the experiment. Observe that certain letters present lower rates of recognition. This is mainly due to the linear deformation imposed on the distance function (13) does not enough deformation

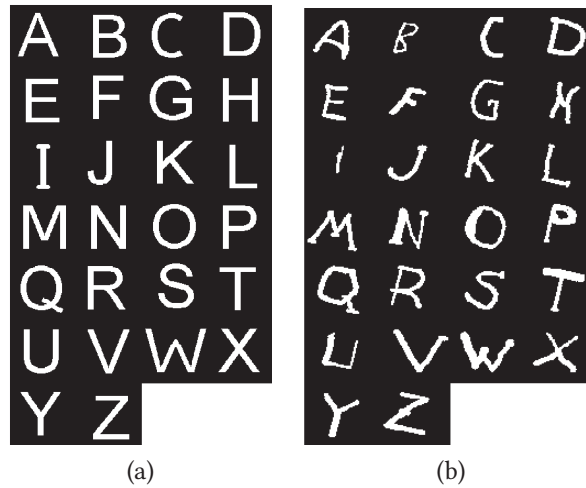


Figure 14. (a) Reference dataset. (b) An example of test dataset.

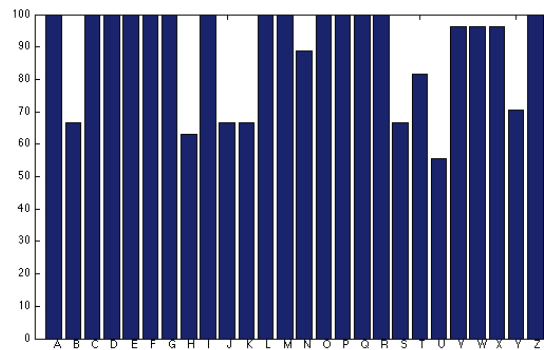


Figure 15. Rate of recognition of letters.

discrimination on terms of measuring the energy of the deformation, and consequently deforming a letter up to being very similar to another letter on the data base. In this case, the proposal can be enriched using a more discriminating nonlinear function. It can also be observed in this experiment, similar to the previous one, it can be observed that the proposal method is problem dependent, i.e., the parameter α and others must to be chosen, in principle, for a specific problem. Although this particularity, it can also be noted that higher values of α improve the performance of the method. This means that the contribution of the CPS to the measure is important for the discriminating process of the method.

20 A. J. Giangreco-Maidana, H. L. Ayala, C. E. Schaerer, W. Villamayor-Venialbo

5. Conclusions

In this paper we introduced a new point descriptor named as Contour point Signature - CPS - which has been proved to have good theoretical properties, as well as invariance to translation, rotation and scale. The CPS induces a distance function metric denoted by $d_{CPS}(\cdot, \cdot)$. The numerical tests of the CPS and its induced metric show that it presents an adequate performance if it is complemented with another metric. In this paper we have used an induced affine transformation metric, and even for this simple metric the results are competitive. Other complementary metrics can be used if the problem requires.

Another important observation is that the choice of the parameters for considering all rotations ($\gamma = 1$) or only part of them ($\gamma < 1$), all points ($\delta = 1$) or only part of them ($\delta < 1$), and the balance between the parts of the metric (α) is problem dependent. This means that the method has to be tuned for each specific problem and in some cases enriched the metric to be used in the discriminating process if it is desired to have very high rate of successes. In general this is true for all methods for the kinds of problems considered in this paper. If however the CPS method is used in its simple form presented in this article, then the method is very competitive and easy to implement computationally.

Acknowledgments

This work was partially supported by CONACYT - Paraguay. H.L.A. acknowledges the support given by 14-INV-202. C.E.S. acknowledges the financial support given by PRONII-CONACYT-Paraguay.

Bibliography

1. T. Adamek and N. E. O'Connor. Efficient contour-based shape representation and matching. In *Proc. 5th ACM SIGMM Int'l Workshop Mult. Inf. Retr.*, MIR '03, pages 138–143, New York, NY, USA, 2003. ACM.
2. T. Adamek and N. E. O'Connor. A multiscale representation method for nonrigid shapes with a single closed contour. *IEEE Trans. Circuits Syst. Video Technol.*, 14(5):742–753, May 2004.
3. A. Amanatiadis, V. Kaburlasos, A. Gasteratos, and S. Papadakis. Evaluation of shape descriptors for shape-based image retrieval. *IET Image Process.*, 5(5):493–499, 2009.
4. X. Bai, X. Yang, L. J. Latecki, W. Liu, and Z. Tu. Learning context-sensitive shape similarity by graph transduction. *IEEE Trans. Pattern Anal. Mach. Intell.*, 32(5):861–874, May 2010.
5. I. Bartolini, P. Ciaccia, and M. Patella. Using the time warping distance for Fourier-based shape retrieval. Tech. Rep. BO-03-02, IEIIT, Nov. 2002.
6. S. Belongie, J. Malik, and J. Puzicha. Shape matching and object recognition using shape contexts. *IEEE Trans. Pattern Anal. Mach. Intell.*, 24(4):509–522, Apr. 2002.
7. D. Conte, P. Foggia, C. Sansone, and M. Vento. Thirty years of graph matching in pattern recognition. *Int'l J. Patt. Recogn. Artif. Intell.*, 18(3):265–298, 2004.
8. T. F. Cootes, C. J. Taylor, D. H. Cooper, and J. Graham. Active shape models – Their training and application. *Computer Vision and Image Understanding*, 61(1):38–59, Jan. 1995.
9. D. Doermann, E. Rivlin, and I. Weiss. Logo recognition using geometric invariants. In *Document Analysis and Recognition*, pages 894–897, 1993.
10. D. Doermann, E. Rivlin, and I. Weiss. Applying algebraic and differential invariants for logo recognition. *Mach. Vis. Appl.*, 9(2):73–86, 1996.

11. S. Fan. Shape representation and retrieval using distance histograms. Technical Report TR 01-14, Department of Computer Science, University of Alberta, Edmonton, Alberta, Canada, Oct. 2001.
12. J. Flusser. Object matching by means of matching likelihood coefficients. *Pattern Recognit. Lett.*, 16:893–900, 1995.
13. J. Flusser and T. Suk. Pattern recognition by affine moment invariants. *Pattern Recognit.*, 26(1):167–174, May 1993.
14. A. Ghosh and N. Petkov. Effect of high curvature point deletion on the performance of two contour based shape recognition algorithms. *Int'l J. Patt. Recogn. Artif. Intell.*, 20(6):913–924, 2006.
15. E. S. Gollin. Developmental studies of visual recognition of incomplete objects. *Percep. Motor Skills*, 11:289–298, 1960.
16. C. Gope, N. Kehtarnavaz, G. Hillman, and B. Würsig. An affine invariant curve matching method for photo-identification of marine mammals. *Pattern Recognit.*, 38:125–132, 2005.
17. M. K. Hu. Visual pattern recognition by moment invariants. *IRE Trans. Information Theory*, 8:179–187, 1962.
18. K. Kpalma and J. Ronsin. An overview of advances of pattern recognition systems in computer vision. In G. Obinata and A. Dutta, editors, *Vision Systems: Segmentation and Pattern Recognition*, chapter 10, pages 169–194. I-Tech (Advanced Robotic Systems), May 2007.
19. L. J. Latecki and R. Lakämper. Shape similarity measure based on correspondence of visual parts. *IEEE Trans. Pattern Anal. Mach. Intell.*, 22(10):1185–1190, Oct. 2000.
20. D. Li and S. Simske. Shape retrieval based on distance ratio distributions. HP Tech Report HPL-2002-251, Intelligent Enterprise Technologies Laboratory, HP Laboratories Palo Alto, Sept. 2002.
21. S. Loncaric. A survey of shape analysis techniques. *Pattern Recognit.*, 31(8):983–1001, 1998.
22. E. Miliou and E. G. M. Petrakis. Shape retrieval based on dynamic programming. *IEEE Trans. Image Process.*, 9(1):141–147, Jan. 2000.
23. G. Mori, S. Belongie, and J. Malik. Efficient shape matching using shape contexts. *IEEE Trans. Pattern Anal. Mach. Intell.*, 27(11):1832–1837, Nov. 2005.
24. H. S. Nagendraswamy and D. S. Guru. A new method of representing and matching two dimensional shapes. *International Journal of Image and Graphics*, 7:337 – 405, 2007.
25. J. Peng and B. Bhanu. Local discriminative learning for pattern recognition. *Pattern Recognit.*, 34:139–150, 2001.
26. E. G. Petrakis, A. Diplaros, and E. Miliou. Matching and retrieval of distorted and occluded shapes using dynamic programming. *IEEE Trans. Pattern Anal. Mach. Intell.*, 24(11):1501–1516, Nov. 2002.
27. R. Polikar. Pattern recognition. In *Wiley Encyclopedia of Biomedical Engineering*. John Wiley & Sons, Inc., 2006.
28. P. V. M. Rao, P. Bodas, and S. G. Dhande. Shape matching of planar and spatial curves for part inspection. *Computer-Aided Design & Applications*, 3(1–4):289–296, 2006.
29. H. Riemenschneider, M. Donoser, and H. Bischof. Using partial edge contour matches for efficient object category localization. In *Proc. Eur. Conf. Comp. Vision*, number 11th ECCV: Part V in ECCV'10, pages 29–42, Berlin, Heidelberg, 2010. Springer-Verlag.
30. L. Schomaker, E. de Leau, and L. Vuurpijl. Using pen-based outlines for object-based annotation and image-based queries. In D. Huijsmans and A. Smeulders, editors, *Proc. Int'l Conf. Visual Inf. and Inf. Sys.*, volume 1614 of *VISUAL '99*, pages 585–592. Springer Berlin / Heidelberg, June 1999.
31. C. Sheng and Y. Xin. Shape-based image retrieval using shape matrix. *Int'l J. Signal Process.*, 1(3):163–166, 2005.
32. K. Siddiqi, A. Shokoufandeh, S. J. Dickinson, and S. W. Zucker. Shock graphs and shape matching. *Int. J. Comput. Vision*, 35:13–32, Nov. 1999.

- 1
2
3
4
5
6
7
8
9
10
11
12
13
14
15
16
17
18
19
20
21
22
23
24
25
26
27
28
29
30
31
32
33
34
35
36
37
38
39
40
41
42
43
44
45
46
47
48
49
50
51
52
53
54
55
56
57
58
59
60
61
62
63
64
65
- 22 A. J. Giangreco-Maidana, H. L. Ayala, C. E. Schaerer, W. Villamayor-Venialbo
33. T. Suk and J. Flusser. Graph method for generating affine moment invariants. In *Proc. Int'l Conf. Patt. Recogn.*, pages 192–195. IEEE, 2004.
34. R. C. Veltkamp. Shape matching: Similarity measures and algorithms, invited talk. In *Proc. Int'l Conf. Shape Model. Appl.*, pages 188–197, Genova, Italy, May 2001.
35. R. C. Veltkamp and M. Hagedoorn. State-of-the-art in shape matching. Technical Report UU-CS-1999-27, Utrecht University, Department of Computing Science, Utrecht, The Netherlands, 1999.
36. R. C. Veltkamp and L. J. Latecki. Properties and performance of shape similarity measures. In H. H. Bock, W. Gaul, M. Vichi, P. Arabie, D. Baier, F. Critchley, R. Decker, E. Diday, M. Greenacre, C. Lauro, J. Meulman, P. Monari, S. Nishisato, N. Ohsumi, O. Opitz, G. Ritter, M. Schader, C. Weihs, V. Batagelj, H.-H. Bock, A. Ferligoj, and A. Žiberna, editors, *Data Science and Classification*, Studies in Classification, Data Analysis, and Knowledge Organization, pages 47–56. Springer Berlin Heidelberg, 2006.
37. R. C. Veltkamp and M. Tanase. Content-based image retrieval systems: A survey. Technical Report UU-CS-2000-34, Department of Computing Science, Utrecht University, 2000. (extended version 2002).
38. W. Villamayor-Venialbo, H. Legal-Ayala, E. Justino, and J. Facon. A partial matching framework based on set exclusion criteria. *International Journal of Pattern Recognition and Artificial Intelligence*, 26(2):1–37, 2012.
39. B. Wang and Y. Q. Chen. An invariant shape representation: interior angle chain. *International Journal of Pattern Recognition and Artificial Intelligence*, 21(3):543 – 559, 2007.
40. J. Xie, P.-A. Heng, and M. Shah. Shape matching and modeling using skeletal context. *Pattern Recognit.*, 41:1756–1767, 2008.
41. M. Yang, K. Kpalma, and J. Ronsin. A survey of shape feature extraction techniques. In P.-Y. Yin, editor, *Pattern Recognition Techniques, Technology and Applications*, chapter 3, pages 43–90. I-Tech, Nov. 2008.
42. M. Yang, K. Kpalma, and J. Ronsin. Chord context algorithm for shape feature extraction. *Object Recognition.*, pages 65–82, 2011.
43. D. S. Zhang and G. Lu. A comparative study of Fourier descriptors for shape representation and retrieval. In *Proc. Asian Conf. Comp. Vision*, 2002.
44. D. S. Zhang and G. Lu. A comparative study of curvature scale space and Fourier descriptors for shape-based image retrieval. *Visual Communication and Image Representation*, 14(1):39–57, Mar. 2003.
45. D. S. Zhang and G. Lu. Review of shape representation and description techniques. *Pattern Recognit.*, 37(1):1–19, 2004.



Campus de la UNA
SAN LORENZO-PARAGUAY

UNIVERSIDAD NACIONAL DE ASUNCIÓN FACULTAD POLITÉCNICA

January 4, 2017, San Lorenzo, Paraguay

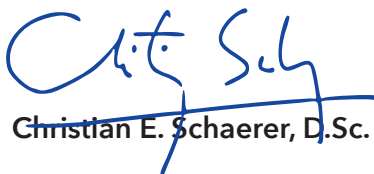
David Zhang
Department of Computing
Hong Kong Polytechnic University
Kowloon, Hong Kong
Tel: +852 2766 7271
Fax: +852 2774 0842
Email: csdzhang@comp.polyu.edu.hk

Dear Prof. Zhang,

In attachment you will find the manuscript entitled: "CONTOUR-POINT SIGNATURE SHAPE DESCRIPTOR FOR POINT CORRESPONDENCE" which is co-authored with Alejandro J. Giangreco Maidana, Horacio Legal Ayala, and Waldemar Villamayor-Venialbo.

In this manuscript, we introduce a novel signature denoted by CPS, which can be applied in several situations. We made an effort in presenting the mathematical properties of CPS in order to give an adequate theoretical framework for future research, even in broader contexts. We consider that a new mathematical paradigm based on signatures is introduced through CPS for image processing.

Yours Faithfully,



Christian E. Schaerer, D.Sc.

Polytechnic School
National University of Asuncion
San Lorenzo, Paraguay

Email: cschaer@pol.una.py
Cel-Phone: +595-982-651880